Anchoring of $NiCo_x$ Alloy Nanoparticles on Nitrogen Vacancy-Rich Carbon Nitride Nanotubes toward Promoting Efficiently Photocatalytic CO_2 Conversion into Solar Fuel

Qingqing Zhang[*,a,†], *Bo Tao*[b, †], *Chen Zhao*[a], *Zongyan Zhao,*[*,c] *Hui Wu*[a], *Xiaohui Zhong*[a], *Zhigang Zou*[b,d] *and Yong Zhou*[*,a,b,d]

[a.] School of Chemical and Environmental Engineering, Anhui Polytechnic University, Wuhu, Anhui, 241000, P. R. China.

[b.] Key Laboratory of Modern Acoustics (MOE), Institute of Acoustics, School of Physics, National Laboratory of Solid State Microstructures, Collaborative Innovation Center of Advanced Microstructures, Eco-Materials and Renewable Energy Research Center (ERERC), Jiangsu Key Laboratory for Nano Technology, Nanjing University, Nanjing, Jiangsu, 210093, P. R. China.

[c.] Faculty of Materials Science and Engineering, Kunming University of Science and Technology, Kunming 650093, P. R. China. Email: zzy@kust.edu.cn

[d.] School of Science and Engineering, The Chinese University of Hongkong (Shenzhen), Shenzhen, Guangdong, 518172, P. R. China.

* Correspondence: zhouyong1999@nju.edu.cn

† These authors contributed equally to this work.

1. Experimental Details

Chemicals and Materials: Melamine ($C_3H_6N_6$, Sigma-Aldrich, 99%), nitric acid (HNO_3, Nanjing Chemical Reagent Co., Ltd., 68%), ethylene glycol ($C_2H_6O_2$, Sigma-Aldrich, 99%), nickel nitrate hexahydrate ($Ni(NO_3)_2·6H_2O$, Sigma-Aldrich, 99%), and cobaltous nitrate hexahydrate ($Co(NO_3)_2·6H_2O$, Sigma-Aldrich, 99%) were used as received without any purification.

***Synthesis of V_N-CNNTs*:** Nitrogen vacancy-rich carbon nitride nanotubes (V_N-CNNTs) were synthesized *via* calcination protonated melamine precursors that resulted from morphological transformation of melamine in nitric acid. Typically, melamine (4 g) was dissolved into ethylene glycol (100 mL) under 100 °C. Afterword, HNO_3 was dropwise added into the solution. After reaction, the produced white precipitates were collected by centrifugation, rinsed with ethanol, and dried at 80 °C overnight, resulting in protonated melamine precursors. The as-prepared protonated melamine precursors were calcined at 550 ºC for 2 h with a heating rate of 2 ºC min^{-1} under an Ar flow, and cooled down naturally, achieving a yellow product. The synthesized materials were labeled as V_N-CNNTs. For comparison, bulk carbon nitride (BCN) was directly synthesized by calcinating melamine at 550 ºC for 2 h.

Synthesis of NiCo/V_N-CNNTs: NiCo alloy nanoparticles (NPs) were deposited on V_N-CNNTs with a modulatory loading weights of alloy NPs to V_N-CNNTs through a facile chemical reduction method. Typically, V_N-CNNTs (0.5 g) was dispersed in 100 mL ethanol. Subsequently, stoichiometric amounts of $Ni(NO_3)_2·6H_2O$ and $Co(NO_3)_2·6H_2O$ (mole ratio of Ni:Co from 0.2 to 0.6) were dissolved in the ethanol solution, followed by stirring in an ice-bath for 2 h. Afterward, the excess $NaBH_4$ (0.1 mol L^{-1}) was added into the mixture and stirring for 12 h. The final products were collected by washing with water and ethanol and dried at 80 ºC under vacuum condition. The obtained materials were denoted as $NiCo_x/V_N$-CNNTs, where x represented the molar ratio of Ni to Co (x = 0.2–0.6). For comparison, the contrast samples of Ni/V_N-CNNTs and Co/V_N-CNNTs were fabricated according to the same method with $NiCo_{0.4}/V_N$-CNNTs except that $Co(NO_3)_2·6H_2O$ or $Ni(NO_3)_2·6H_2O$ were not added.

***Characterization*:** Transmission electron microscope (TEM) images were collected on a JEOL 3010 microscope operated at 300 kV. The specific surface area was measured by nitrogen adsorption-desorption using Micromeritics TriStar specific surface area analyzer operating at 77 K and calculated by Brunauer-Emmett-Teller (BET) method. Power X-ray diffraction patterns (XRD) were recorded on a Rigaku

Ultima III diffractometer using a Cu Kα X-ray radiation. Fourier transform infrared spectra (FTIR) were collected on a Nicolet Nexus-870 FTIR spectrometer with KBr pellets. X-ray photoelectron spectroscopy (XPS) was obtained by Thermo Fisher Scientific ESCALAB 250 X-ray photoelectron spectrometer with an Al Kα X-ray source, and the binding energy was standardized using the adventitious C1s peak at 284.6 eV. Ultraviolet–visible spectrophotometer (UV–vis) was hired to record the UV-visible diffuse reflectance spectra on Shimadzu UV-2550 and switched to the absorption spectrum on the basis of the Kubelka−Munk connection at room temperature. Steady-state photoluminescence (PL) spectra were obtained with PerkinElmer LS55 fluorescence spectrometer. Electron paramagnetic resonance (EPR) spectra were collected from the EMX 10/12 EPR spectrometer operating at 9.788 GHz.

***Photoelectrochemical Measurements*:** All photoelectrochemical measurements were conducted in an electrochemical workstation (CHI-660E, shanghai Chen Hua Co., Ltd.) with a three-electrode cell system, in which fluorine-tin oxide (FTO) glass carbon electrode, Pt wire, and saturated Ag/AgCl serving as working electrode, counter electrode, and reference electrode, respectively. The working electrode was prepared by dispersing 30 mg photocatalyst in 30 mL acetone, followed by 15 mg iodine. The suspension liquid was evenly deposited on the 1 cm^2 FTO glass electrode by electrophoresis and dried naturally at room temperature.

Computational Details: All calculations were based on density functional theory and performed using the Cambridge Serial Total Energy Package (CASTEP) codes, employing the on-the-fly ultrasoft pseudopotential. The Perdew-Burke-Ernzerhof (PBE) exchange-correlation functional at the generalized gradient approximation (GGA) level was utilized. The Kohn-Sham wave functions of the valence electrons were described by a plane-wave basis set with an energy cutoff of 570 eV. For geometric optimization, the Broyden-Fletcher-Goldfarb-Shanno (BFGS) scheme was selected as the minimization algorithm. The Monkhorst-Pack scheme was applied for the K-points grid sampling with a setting of 5 × 5 × 1 for the irreducible Brillouin zone. The atomic coordinates were optimized to achieve accurate geometry, and the convergence criteria for structure optimizations were defined as follows: a maximum force tolerance of 0.03 eV/Å, a maximum stress tolerance of 0.05 GPa, a maximum displacement tolerance of 1×10^{-3} Å, and a maximal energy change per atom of 1×10^{-5} eV. Meanwhile, the self-consistent field tolerance was set to 5×10^{-7} eV/atom. To obtain a more precise electronic structure, the HSE06 hybrid functional was employed

for the calculation based on the optimized structure. In order to accurately calculate the van der Waals interaction between two layers, we used the Grimme dispersion correction method in DFT-D.

In this work, we initiated by optimizing the bulk model of C_3H_4, yielding the following crystalline parameters: a = 7.148 Å, b = 12.397 Å, c = 24.748 Å. Subsequently, we exfoliated a monolayer of g-C_3N_4 from 2×1×1 supercell, and removed a nitrogen atom from it, resulting in the V_N-C_3H_4 model (total atom: 55) with 20-Å-thickness vacuum layer. NiCo alloy nanoparticles were constructed based on optimized FCC-Ni metal. The adsorption position of reactants was determined by simulated annealing method. To gain insight into the CO_2 adsorption and activation, we have employed first-principles simulation to examine the CO_2 adsorption on the surface of NiCo alloy nanoparticles. The stable adsorption sites of CO_2 and active reaction sites of CO_2-to-CH_4 conversion are Co atoms.

2. Characterizations

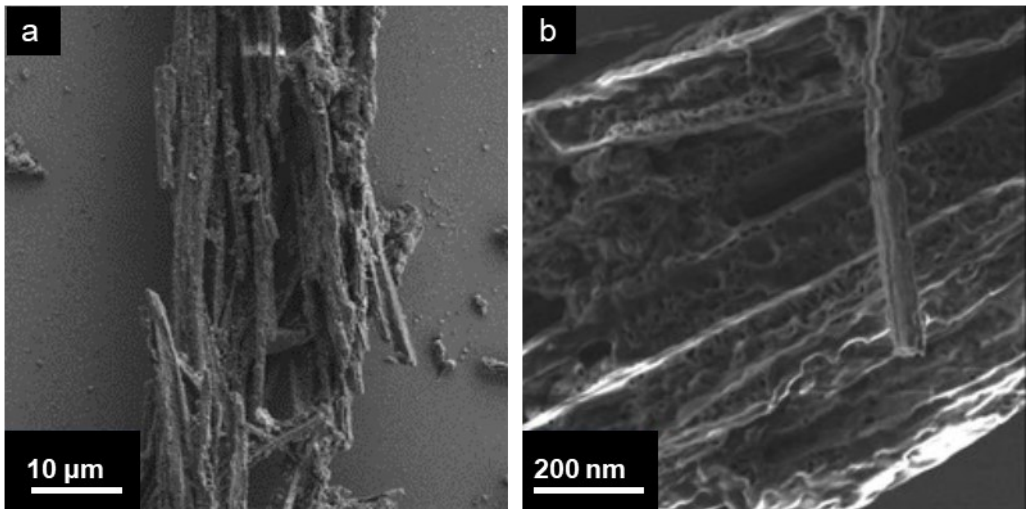

Fig. S1 (a-b) SEM images of V_N-CNNTs.

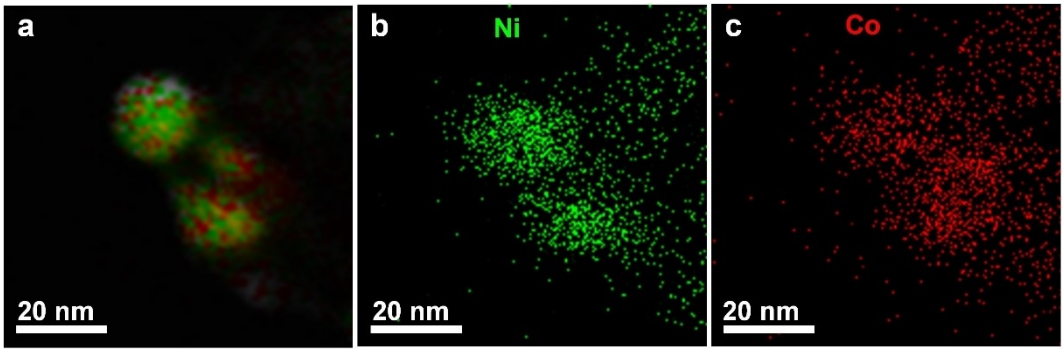

Fig. S2 (a) STEM and the corresponding (b-c) EDS-mapping images of $NiCo_{0.4}/V_N$-CNNTs.

1

2

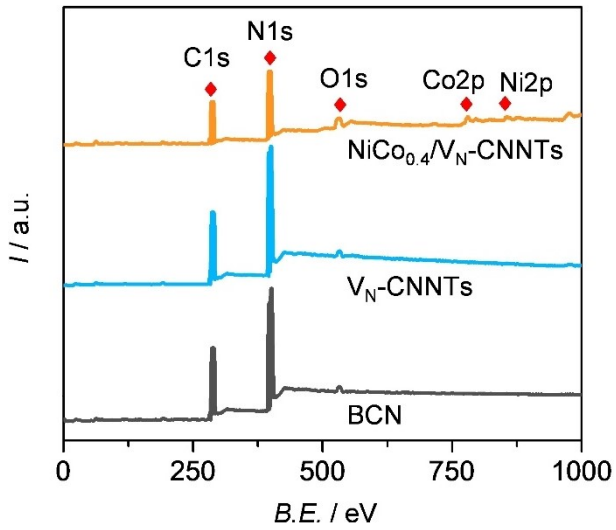

Fig. S3 XPS survey spectra of BCN, V_N-CNNTs and $NiCo_{0.4}/V_N$-CNNTs.

1

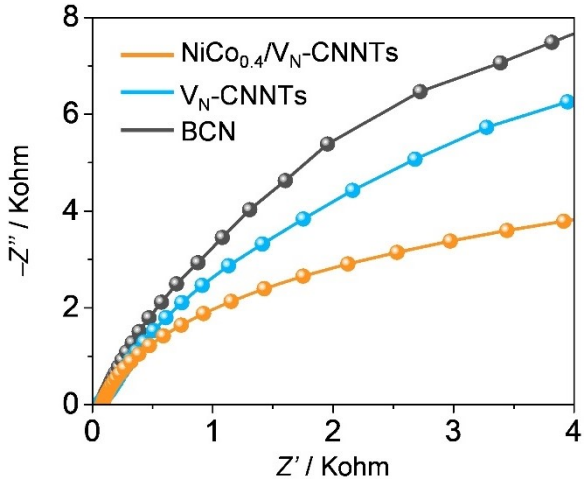

Fig. S4 The electrochemical impedance spectra of BCN, V_N-CNNTs and $NiCo_{0.4}/V_N$-CNNTs.

Table S1 The reported bimetallic catalytic systems in photocatalytic CO_2 reduction and their corresponding ratio of CH_4/CO evolution rate.

Entry	Catalyst	Light	Oxidant	r_{CH_4}/r_{CO}	Ref.
1	Mn_1Co_1/CN	300 W Xe lamp	H_2O	0.01	*Angew. Chem. Int. Edit.* **2022**, *61*, e202206579.
2	Ni/Mn-Oxo/g-C_3N_4	300 W Xe lamp	H_2O	0.16	*Sol. RRL* **2021**, *5*, 2000472.
3	$Co_1Ag_{(1+n)}$/PCN	300 W Xe lamp	H_2O	0.11	*ACS Nano* **2023**, *17*, 11869.
4	g-C_3N_4 –$Co_{1.6}Ni_{0.4}$	300 W Xe lamp	H_2O	0.09	*J. Colloid Interf. Sci.* **2022**, *625*, 722.
5	PtCu-crCN	300 W Xe lamp	H_2O	0.24	*Chinese J Catal.* **2022**, *43*, 451.
6	CoRu-HCNp	300 W Xe lamp	H_2O	0.09	*Adv. Mater.* **2021**, *33*, 2105135.
7	1Cu-1Mn/mCN	300 W Xe lamp	H_2O	0.13	*Appl. Surf. Sci.* **2019**, *492*, 125.
8	Pd_1-Cu_1/CN	300 W Xe lamp	H_2O	0.09	*Small*, **2024**, *20*, 2308767.
9	$NiCo_{0.4}/V_N$-CNNTs	300 W Xe lamp	H_2O	0.56	This work